REPORT DOCUMENTATION PAGE

Form Approved
OMB No. 0704-0188

1. REPORT DATE *(DD-MM-YYYY)*	2. REPORT TYPE	3. DATES COVERED *(From - To)*
30-Sep-2009	REPRINT	

4. TITLE AND SUBTITLE
WAVE PROPAGATION FROM COMPLEX 3D SOURCES USING THE REPRESENTATION THEOREM

5a. CONTRACT NUMBER
FA8718-08-C-0010

5b. GRANT NUMBER

5c. PROGRAM ELEMENT NUMBER
62601F

6. AUTHOR(S)
Jeffry L. Stevens and Heming Xu

5d. PROJECT NUMBER
1010

5e. TASK NUMBER
SM

5f. WORK UNIT NUMBER
A1

7. PERFORMING ORGANIZATION NAME(S) AND ADDRESS(ES)

Science Applications International Corporation
10260 Campus Point Drive
San Diego, CA 92121-1152

8. PERFORMING ORGANIZATION REPORT NUMBER

9. SPONSORING / MONITORING AGENCY NAME(S) AND ADDRESS(ES)
Air Force Research Laboratory
29 Randolph Road
Hanscom AFB, MA 01731-3010

10. SPONSOR/MONITOR'S ACRONYM(S)
AFRL/RVBYE

11. SPONSOR/MONITOR'S REPORT NUMBER(S)
AFRL-RV-HA-TR-2009-1076

12. DISTRIBUTION / AVAILABILITY STATEMENT
Approved for Public Release; Distribution Unlimited.

13. SUPPLEMENTARY NOTES
Reprinted from: Proceedings of the 2009 Monitoring Research Review – Ground-Based Nuclear Explosion Monitoring Technologies, 21 – 23 September 2009, Tucson, AZ, Volume III pp 574 - 581.

14. ABSTRACT
In spite of extensive prior research on generation of seismic waves hy underground nuclear explosions, it is still not possible to provide a complete explanation for the observed wavefields, particularly at regional distances. Spherically symmetric explosion models embedded in layered elastic media effectively model the *P* phases generated by explosions, and the major characteristics of some reflected and transmitted phases. Nonlinear axisymmetric finite difference calculations of explosions including gravity and the effect of the free surface can model a more realistic explosion source that directly generates shear waves. These models explain more characteristics of explosion-generated seismic waves, including some aspects of regional shear phases. However, it is clear that linear and nonlinear near-source 3D effects are important in many cases. *SH* waves are commonly observed within a few km of explosions, too close to have been generated by (simple) conversion of vertical and radial components, and often larger than those components. Furthermore, it has not been established what impact 3D effects have on discriminants and on explosion yield estimates. It is important, therefore, to he ahle to model and understand how 3D source and source region heterogeneity affect the seismic wavefield, and what impact this has on parameters used for nuclear monitoring.

To test the code, we have performed calculations using cavities of three shapes: spherical, rectangular and elliptical, each with the same volume. An explosion with the same yield was detonated inside each cavity. We compare the solutions from these three cavity explosions in the near field and at distance. Gravity is included in the calculations, and we start with an equilibrium solution obtained by running the finite-element CRAM3D with overburden pressure only, prior to the start of the explosion calculation. Nonlinear deformation is seen around the cavity. The results show very good agreement between 2D and 3D solutions at distance for the spherical cavity explosion. Nonspherical wave components from nonspherical rectangular and elliptical cavities are clearly seen in the near field. The rectangular cavity shows more pronounced tangential motion than the elliptical cavity away from axes of symmetry.

15. SUBJECT TERMS
Explosion sources, Hybrid synthetic Seismograms, Explosion effects prediction

16. SECURITY CLASSIFICATION OF:			17. LIMITATION OF ABSTRACT	18. NUMBER OF PAGES	19a. NAME OF RESPONSIBLE PERSON
a. REPORT	b. ABSTRACT	c. THIS PAGE			Robert J. Raistrick
UNCLAS	UNCLAS	UNCLAS	SAR	8	19b. TELEPHONE NUMBER *(include area code)*

WAVE PROPAGATION FROM COMPLEX 3D SOURCES USING THE REPRESENTATION THEOREM

Jeffry L. Stevens and Heming Xu

Science Applications International Corporation

Sponsored by the Air Force Research Laboratory

Contract No. FA8718-08-C-0010
Proposal No. BAA08-57

ABSTRACT

In spite of extensive prior research on generation of seismic waves by underground nuclear explosions, it is still not possible to provide a complete explanation for the observed wavefields, particularly at regional distances. Spherically symmetric explosion models embedded in layered elastic media effectively model the *P* phases generated by explosions, and the major characteristics of some reflected and transmitted phases. Nonlinear axisymmetric finite difference calculations of explosions including gravity and the effect of the free surface can model a more realistic explosion source that directly generates shear waves. These models explain more characteristics of explosion-generated seismic waves, including some aspects of regional shear phases. However, it is clear that linear and nonlinear near-source 3D effects are important in many cases. *SH* waves are commonly observed within a few km of explosions, too close to have been generated by (simple) conversion of vertical and radial components, and often larger than those components. Furthermore, it has not been established what impact 3D effects have on discriminants and on explosion yield estimates. It is important, therefore, to be able to model and understand how 3D source and source region heterogeneity affect the seismic wavefield, and what impact this has on parameters used for nuclear monitoring.

We are in the second year of a project to develop and test a three-dimensional nonlinear finite element code CRAM3D, which will be used to calculate nonlinear explosion sources that have both 3D source geometry and may occur in a 3D heterogeneous medium. The code includes the same well-tested material models that have been used in earlier axisymmetric calculations. In addition, we are developing algorithms based on the representation theorem to propagate the motion from these source region calculations to any desired distance. We have implemented a technique that allows us to propagate the results of near source 3D finite element calculations to regional and teleseismic distances. The Green's function and its derivatives are used in conjunction with the numerical solutions on a monitoring surface enclosing the complex source region. Full-waveform solutions at distance, due to complex explosion sources, are computed with the full-waveform Green's function using wavenumber integration; surface wave solutions are computed with the surface wave Green's functions using mode summation; and far field body wave solutions are computed with the outgoing waves from the source region. The excellent agreement in the surface wave portion between the full-wave solutions and surface-wave solutions demonstrates the accuracy of the implementation of the representation theorem and the respective Green's functions and their derivatives.

To test the code, we have performed calculations using cavities of three shapes: spherical, rectangular and elliptical, each with the same volume. An explosion with the same yield was detonated inside each cavity. We compare the solutions from these three cavity explosions in the near field and at distance. Gravity is included in the calculations, and we start with an equilibrium solution obtained by running the finite-element CRAM3D with overburden pressure only, prior to the start of the explosion calculation. Nonlinear deformation is seen around the cavity. The results show very good agreement between 2D and 3D solutions at distance for the spherical cavity explosion. Nonspherical wave components from nonspherical rectangular and elliptical cavities are clearly seen in the near field. The rectangular cavity shows more pronounced tangential motion than the elliptical cavity away from axes of symmetry.

OBJECTIVES

The objective of this project is to investigate the generation of complex seismic waves by explosions in media with 3D heterogeneity using a method based on the exact representation theorem for propagating complex 3D source calculations to local, regional and teleseismic distances.

RESEARCH ACCOMPLISHED

Introduction

Source physics, near source scattering, and propagation effects are all important to understanding seismic phases used in nuclear monitoring. Significant bodies of literature exist that address each subject individually. In addition to extending our understanding of source physics and near source scattering to include the effects of realistic 3D heterogeneity, this project links the progression of energy from its generation by the source, through the near source region, and into its partitioning among local, regional, and teleseismic phases. Distinguishing the far-field *P*- and *S*-waves enables us to quantify the effects of 3D structure on both *P*- and *S*-wave generation. Complete regional waveforms show how this energy is partitioned among the distinct phases, which are important to event detection, identification, and magnitude estimation. How energy is distributed among surface wave modes determines *Lg* amplitudes and *Rg* amplitudes, including near source conversions between these phases. Modal excitation of *Lg* as well as *Rg* has a significant depth dependence that is often neglected in nuclear monitoring studies (Baker et al., 2004), and these amplitudes can be disrupted further by near source effects and source region structure. This can either degrade or improve discrimination capability depending on how well it is understood.

While it is not surprising to observe *SH* waves from any single event, it is surprising to note it is always present; at regional distances, *SH* scales with yield about as well as *P*-waves. While there are many mechanisms, such as near-source scattering, tectonic release, etc. that can generate *SH* waves, all of these effects should be highly variable from one event to the next. To address this question, we need to look at the types of 3D source effects that can exist, the range of variability that would be expected from them, and whether the predictions are consistent with observations.

Source Region Calculations and Propagation Using the Representation Theorem

Our approach is to perform 3D explosion source region calculations, and then to propagate the wavefield to local, regional and teleseismic distances using layered earth Green's functions. We are interested in near-source heterogeneities in both the nonlinear and linear regimes, and therefore require both nonlinear and linear 3D codes to model the source region. In previous projects, we have used two nonlinear codes, STELLAR and CRAM, which are described briefly in Table 1 (we have also used the 1D nonlinear code SKIPPER, which is a spherically symmetric version of CRAM), and the 2D and 3D linear elastic code TRES3D.

Table 1. Numerical simulation tools used in this project

Numerical Simulation Tools	
STELLAR	Eulerian finite difference code. Used to simulate the early time history of the explosion shock. It handles material strength correctly, which is difficult for a Eulerian code. Uses second order accurate Riemann solver scheme. 1D, 2D planar and axisymmetric, and 3D.
CRAM	Lagrangian nonlinear finite difference code. Has been used extensively for axisymmetric explosion calculations. A 3D version of the code is being developed in this project.
TRES3D	Elastic finite difference code. 2D planar and axisymmetric, and 3D.
Elastodynamic Representation Theorem	The time dependent displacements and stresses from 3D source region calculations are saved on a monitoring surface located outside of the region of nonlinear response and/or 3D heterogeneity. A numerical implementation of the representation integral is then used to compute the corresponding far-field seismic radiation.

In past projects, we have used these codes in the following ways:

1. Axisymmetric CRAM was used together with the representation theorem to propagate the results of nonlinear axisymmetric finite difference calculations to regional and teleseismic distances (Day et al., 1987; Stevens et al., 1991; Stevens et al., 2004).
2. Axisymmetric STELLAR was used to calculate the early stages of an explosion. The solution at an appropriate time was overlain onto CRAM to be propagated out to the linear, elastic region. The representation theorem was used to propagate the waveform to regional and teleseismic distances (Rimer et al., 1994). A similar technique was used to overlay results from the Los Alamos National Laboratory code SOIL onto CRAM and propagate the results (Davis et al., 1992).
3. 3D STELLAR was used to calculate near-field waveforms from explosions in rectangular cavities (Stevens et al, 2006).
4. TRES3D was used to calculate the scattering from explosions in a region with 3D heterogeneity and topography (Stevens et al., 2004).

In the current project, we are doing the following: 1) using STELLAR to perform very near source nonlinear 3D calculations and TRES3D to perform linear elastic near source and source region 3D calculations; 2) developing a 3D version of CRAM to model explosions from the source out through the very important nonlinear to linear transition region; and 3) completing the implementation of the elastodynamic representation theorem for full waveforms, modes and body waves.

The technique for propagating numerical calculations using the representation theorem is to save displacements and stresses on a monitoring surface surrounding the nonlinear and/or heterogeneous region of the calculation, and then to convolve these with a Green's function appropriate for the external region (Stevens et al, 1991). In the cases that we have done previously, two-dimensional axisymmetric nonlinear finite difference calculations were performed to model the nuclear explosion, and the stresses and displacements from the calculation were saved on a cylindrical surface in the elastic region outside the region of complex nonlinear behavior. We then invoked the representation theorem and integrated the stresses and displacements with an axisymmetric Green's function to calculate the displacement at any point outside of the calculation. We performed such calculations in 2D, using Green's functions for far-field body waves, for modes and for full regional waveforms using wavenumber integration. The equations for the Green's functions for surface waves are given by Bache et al. (1982). The Green's functions for the complete seismograms are computed using a ring load source, from an algorithm based on the work of Luco and Apsel (1983) and Apsel and Luco (1983). The Green's functions for body waves are generated by a procedure similar to that described by Bache and Harkrider (1976) using a saddle point approximation to calculate a far-field plane wave for a given takeoff angle from a source in a plane-layered medium. Our objective in using multiple types of Green's functions is to gain as much insight as possible into the nature of the seismic wavefield generated by the source. An important part of the current project is to adapt these techniques to propagate seismic waves from 3D source calculations. Although any closed surface can be used for representation theorem integration, we use a cylindrical surface for axisymmetric problems, and a rectangular surface for 3D problems.

3D implementation of the representation theorem

The key to extending the axisymmetric representation theorem discussed above to 3D is to recognize that while the deformation in the source region may be arbitrarily complex, if the structure can be approximated as a plane-layered medium outside of the source region, then the known Green's function for a plane-layered medium applies (this also assumes that we can neglect the interaction of any backscattered waves returning to the source region after leaving it). Note that the representation theorem is exact. That is, no matter how complex the 3D motion is on the source region boundary, it will be correctly propagated by the representation theorem. The following benchmark test demonstrates the performance of the method by comparing the results with equivalent finite difference calculations and wavenumber integration seismograms.

The representation theorem states that displacement at an observation point is made up of contributions due to body forces throughout the source volume, plus contributions due to the traction and displacement on the source volume surface (Aki and Richards, 1980). In the three-dimensional numerical finite difference calculations, we save displacements and stresses due to the seismic source on a monitoring surface on the boundary of a rectangle (five planar surfaces, excluding the upper surface), and calculate Green's functions from each point on the monitoring surface to the receiver and thus, the synthetic seismogram at the receiver point X outside of the monitoring surface is obtained by integrating over the monitoring surface s_M :

$$u_i = \oiint_{S_M} \{G_j^i(\xi;X) * T_j^M(\xi) - u_j^i(\xi) * S_{jk}^i(\xi;X) n_k\} dA \quad (1)$$

in the frequency domain, where $G_j^i(\xi;X)$ and $S_{jk}^i(\xi;X)$ are the Green's function and the stress tensor on the monitoring surface due to a unit impulsive force at X in direction *i*, T_j^M is the traction on the monitoring surface due to the seismic source, *u* is the displacement on the monitoring surface, and *n* is the normal to the monitoring surface. The operator * denotes convolution and the summation convention is assumed.

Equation 1 is applicable to any Green's function for the exterior model, and so we can use a full waveform Green's function, far-field body wave Green's function, and/or modal Green's function as we have discussed earlier for axisymmetric problems. We have implemented this technique for full waveform seismograms calculating the Green's functions using wavenumber integration. We have also implemented the technique for body waves and for modes using corresponding Green's functions.

The synthetic seismograms are computed using the following steps:

1. Displacements and stresses are saved on the monitoring surface during the finite difference calculations.
2. If necessary, the monitoring solutions are resampled onto a coarse grid, as permitted by the required resolution. If there is a symmetry boundary, the entire monitoring surface is constructed first.
3. The finite difference solutions at each point on the monitoring surface are transformed into the frequency domain.
4. The displacement and stress Green's functions due to the three orthogonal forces at the receiver location are calculated for each location on the monitoring surface in the frequency domain (using reciprocity).
5. Equation (1) is used to obtain the solution at the receiver in the frequency domain.
6. The solution is transformed back to the time domain.

Step 5 is implemented with a generalized interface code, which takes as inputs the monitoring wavefields and the Green's functions and stress fields for any of the full-waveforms, surface waves or body waves. Specifically, full-waveform solutions at distance, due to complex explosion sources, are computed with the full-waveform Green's function using wavenumber integration. Surface wave solutions are computed with only with the surface wave Green's functions using mode summation. Far field body wave solutions are computed with the outgoing waves from the source region. The principal advantage of this approach is that it allows us to perform detailed calculations of the source region and then propagate the results to distances that would be impractical or impossible to include in the same numerical calculation. In addition to reducing cost and time, the hybrid method is also more accurate, as numerical dispersion increases with the size and duration of numerical calculations.

Benchmark Tests with Gravity

We have implemented an explicit three-dimensional Lagrangian finite element algorithm that is capable of using multiple processors (Stevens and Xu, 2008). All of the nonlinear material models from 2D CRAM have been implemented and gravity is included. The cavity is placed near the center of the grid and is enclosed by a spider grid which facilitates applying the pressure boundary condition and rezoning elements, as implemented in the two-dimensional axisymmetric code, CRAM.

To test the code, we have performed calculations using three kinds of cavities: spherical (radius 5m), rectangular (each side 8.06m) and elliptical (three axis lengths are 6m, 5m and 4.1667m), each with the same volume. The same yield (0.2kt) explosion is detonated in each cavity. The material external to the cavity is a model for Degelen granite (Stevens et al., 2003). The model consists of two layers: the top layer is 30m thick elastic and the bottom layer is nonlinear. Gravity is included in the calculations, and we start with an equilibrium solution obtained by running the finite-element CRAM3D with overburden pressure only, prior to the start of the explosion calculation. We compare the solutions from these three cavity explosions in the near field and at distance. The shapes of the cavities are shown in Figure 1 and the seismograms in the near field are shown in Figure 2. Each seismogram plot corresponds to a receiver in the same pattern in Figure 1. The radial, tangential and vertical components are represented by red, green and blue lines. The top right plots correspond to the spherical cavity and show no visible tangential motion (green lines) at these receivers. The bottom left plots correspond to the rectangular cavity and show clear tangential motion off the symmetry axes (vertical, horizontal and diagonal). The bottom right plots correspond to the elliptical

cavity and show some visible tangential motion off the symmetry axes (vertical and horizontal). The main waveform characteristics in the elliptical case are quite similar to those in the spherical case.

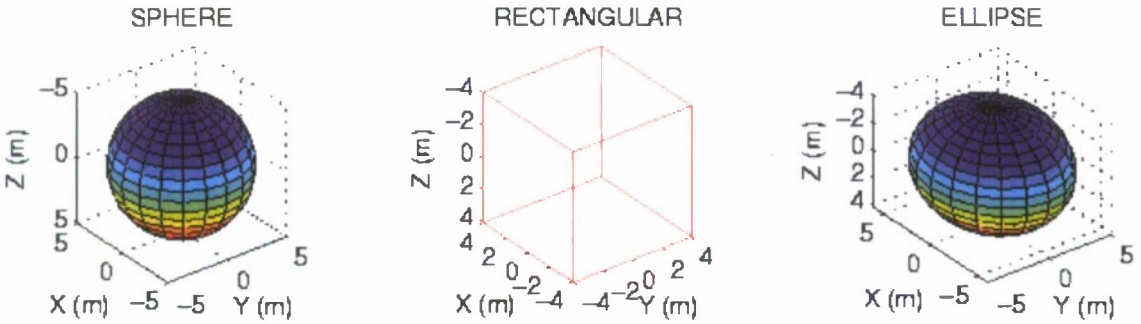

Figure 1. Three cavity shapes with the same volume used for 3D nonlinear explosion calculations.

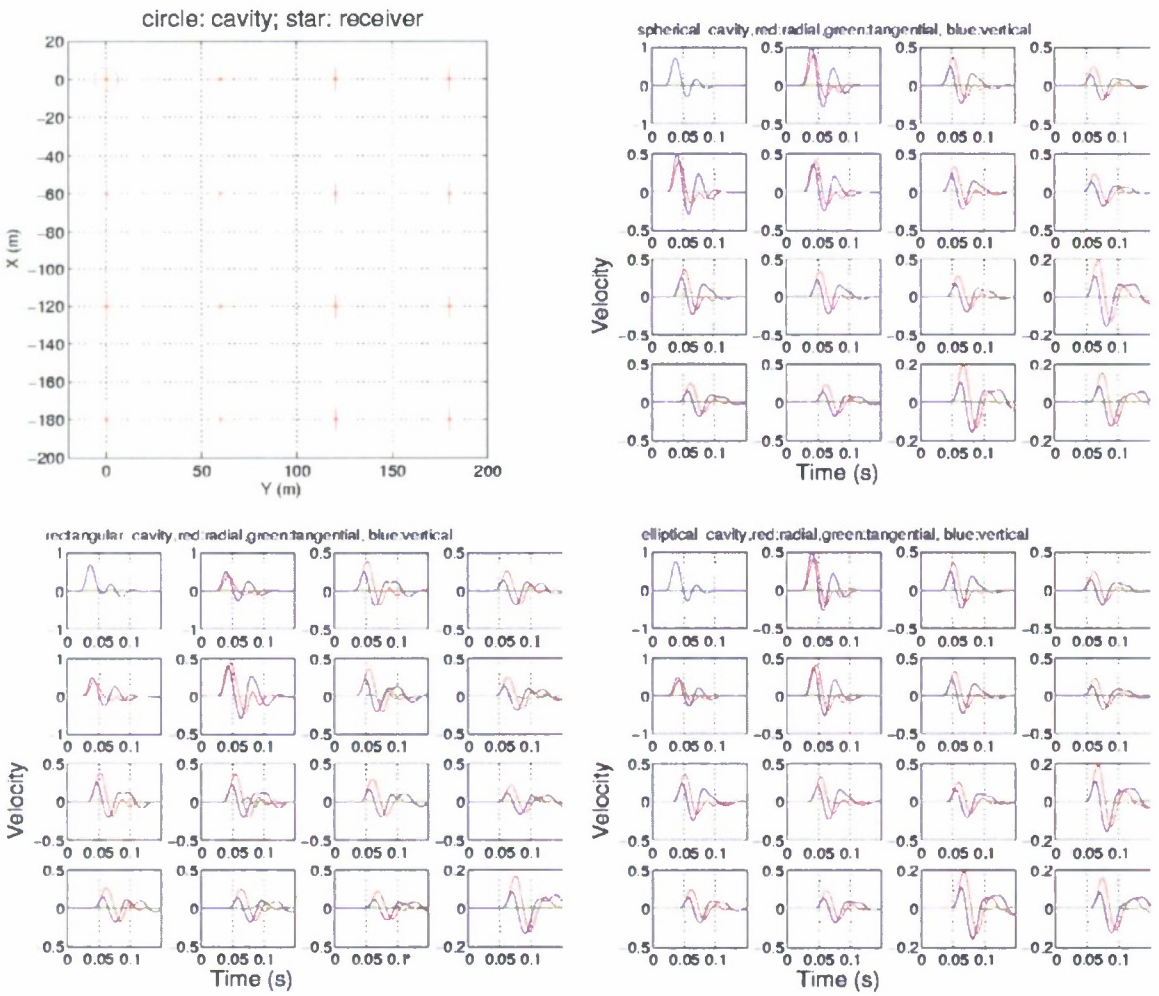

Figure 2. Near field receiver locations (top left): blue circle indicates the cavity location. The near field waveforms due to different cavities are shown at top right and bottom. Red, green and blue lines correspond to radial, tangential and vertical components. Note the tangential components from the non-spherical cavities (bottom two figures).

All the three explosions yield nonlinear deformation around the cavity in Figure 3. The horizontal (top) and vertical (bottom) slices across the cavity center are shown for comparison. Again, both spherical and elliptical cavities show similar patterns but the nonlinear deformation region is enlarged for the rectangular cavity relative to the other two cavities, most likely caused by the effects of the corners.

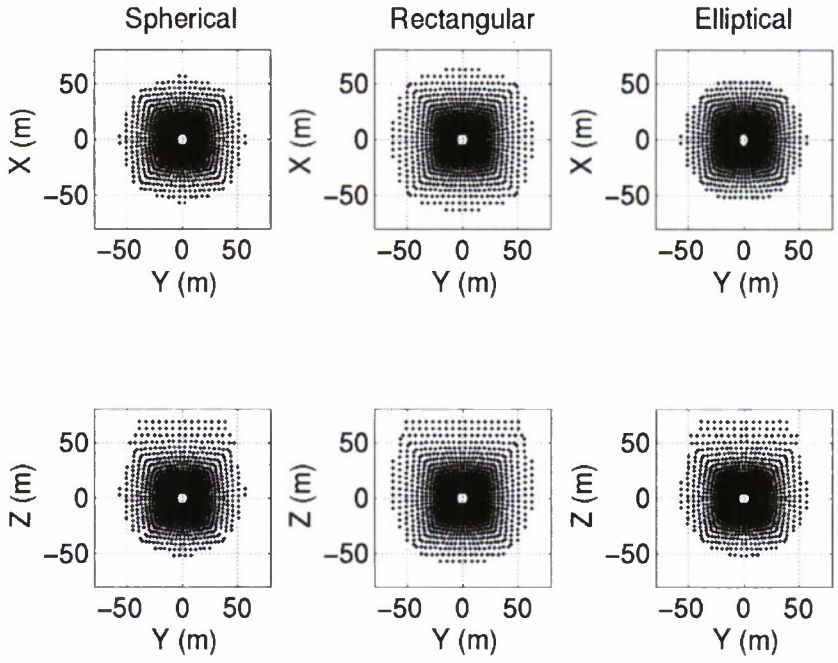

Figure 3. Nonlinear deformation extent around the cavities. The top plots are the horizontal slices across the cavity center and the bottom illustrate vertical slices. The asymmetry in the Z direction is caused by the variation of overburden pressure with depth. More nonlinear deformation occurs above the cavity than below.

Far field solutions are obtained with the representation theorem (Equation 1) by using the displacements and stresses recorded on the monitoring surfaces in the finite-element calculations. An interface code was developed to correctly match the numerical solutions with the Green's functions and the corresponding stresses. We compare the full waveforms and surface waves at two different locations with the same distance. One is at x=2000m,y=1500m (location 1, no symmetry) on the surface and the other at x=2500m and y=0m (location 2 at the symmetry axis). The full waveforms are computed by the wavenumber integration method and the surface waves are computed using mode summation. The results at the two locations for the three cavities are shown in Figure 4. The left corresponds to the location 1 and the right location 2. Each panel has three components. The red and green lines indicate the full waveform solutions and surface wave solutions, respectively, and the blue dashed lines, the 2D full waveform solutions in the spherical cavity case. All the waveforms are low pass filtered below 5Hz. It is clearly seen that the mode summation solutions (green lines, Figure 4) match the surface wave portions of the full waveform solutions (red lines, Figure 4) for all the cavity types at two locations very well. For the spherical cavity full-waveform solutions, there is also very good agreement between 2D (blue dashed lines, Figure 4) and 3D, validating the proper implementation of the Lagrangian finite-element algorithms and the representation theorem in 3D. It is also noted that the spherical and elliptical cavities have the similar waveforms at distance, as in the near field. The wave amplitudes are slightly larger for the rectangular cavity (center row, Figure 4) and consistent with nonlinear deformation extent. The tangential motions are very small for the three cavities and indicate that the source asymmetry due to a small yield, as seen in the horizontal nonlinear deformation distribution (top row, Figure 4), is quite weak at low frequencies, which is also verified by comparing the waveform solutions at the two locations.

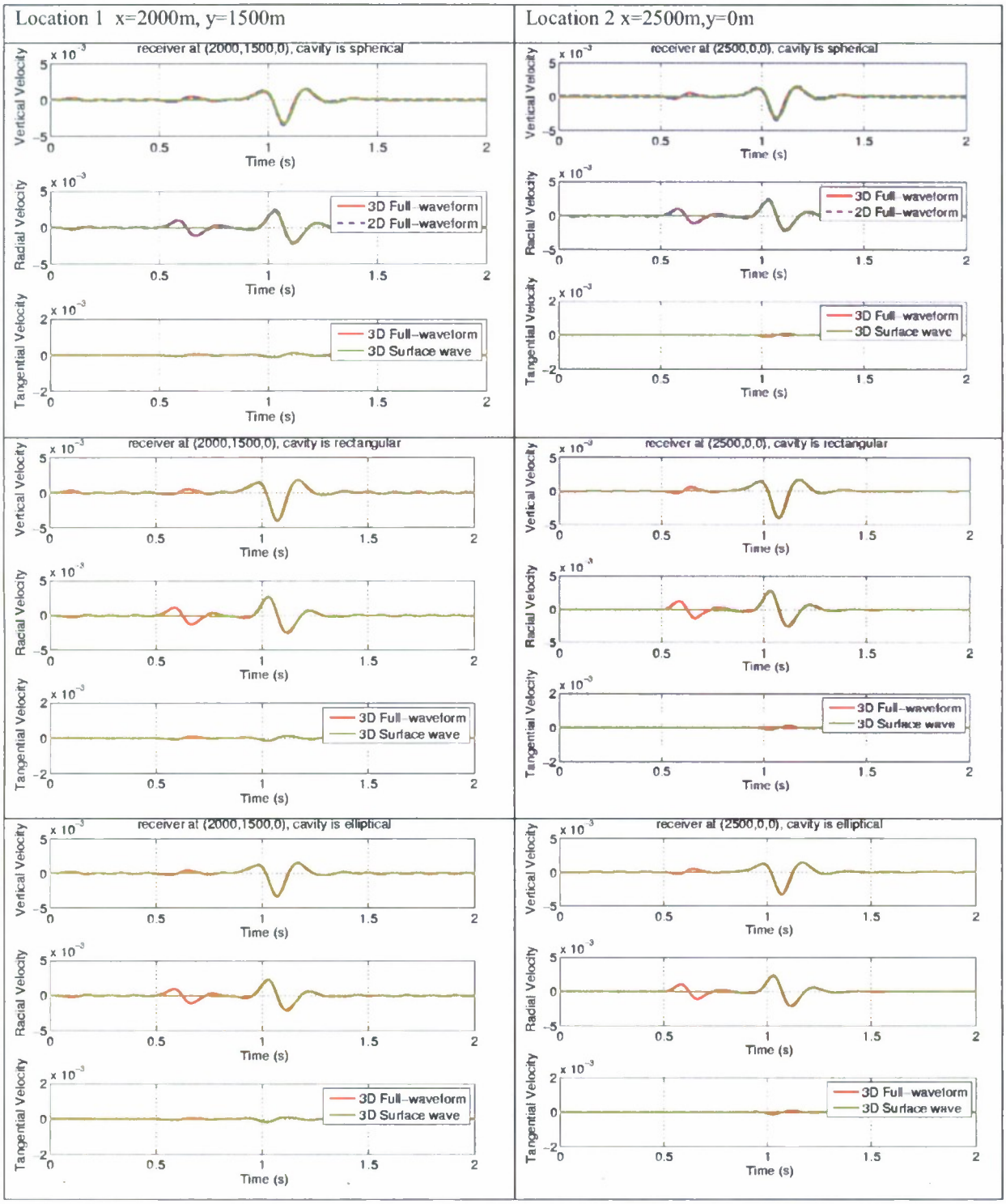

Figure 4. Far field waveforms using the wavenumber integration method and mode summation. Waveforms at location 1 are shown on the left, location 2 on the right. There is excellent agreement between the full-waveform solutions and surface wave solutions for the surface wave part of the waveform. Excellent agreement is also demonstrated for the full waveform solutions in 2D (blue dashed lines) and 3D (top).

CONCLUSIONS AND RECOMMENDATIONS

We are in the second year of a project to understand 3D effects on seismic radiation from underground nuclear explosions. We have nearly completed development of a 3D version of CRAM, the Lagrangian code we have used previously for performing axisymmetric calculations of underground explosions. We have also implemented an interface code, which utilizes any Green's functions in order to propagate the results of the near field 3D calculations to regional and teleseismic distances using the representation theorem. The objectives are to complete implementation of the numerical methods and then perform 3D calculations to understand and model the effects of 3D source region heterogeneity and the seismic response to it in a realistic source scenario.

REFERENCES

Aki, K. and P. G. Richards (1980). *Quantitative Seismology -- Theory and Methods*, W. H. Freeman and Company, San Francisco, CA.

Apsel, R. J. and J. E. Luco (1983). On the Green's Functions for a Layered Half-Space, Part II, *Bull. Seism. Soc. Am.* 73: 931–951.

Bache, T. C. and D. G. Harkrider (1976). The Body Waves Due to a General Seismic source in a Layered Earth Model, *Bull. Seism. Soc. Am.* 66: 1805–1819.

Bache, T. C., S. M. Day and H. J. Swanger (1982). Rayleigh Wave Synthetic Seismograms from Multi-Dimensional Simulations of Underground Explosions, *Bull. Seism. Soc. Am.* 72: 15–28.

Baker, G. E., J. L. Stevens and H. Xu (2004), *Lg* Group Velocity: A Depth Discriminant Revisited, *Bull. Seism. Soc. Am.* 94: 722–739.

Davis, C. G., W. E. Johnson, J. L. Stevens, N. Rimer, T. G. Barker, E. J. Halda, E. Bailey, and W. Proffer (1992). Seismic signals from asymmetric radiation-hydrodynamic calculations, Los Alamos National Laboratory report LA-12506-MS.

Day, S. M., J. T. Cherry, N. Rimer and J. L. Stevens (1987). Nonlinear model of tectonic release from underground explosions, *Bull. Seism. Soc. Am.* 77: 996–1016.

Luco, J. E. and R. J. Apsel (1983). On the Green's Functions for a Layered Half-Space, Part I, *Bull. Seism. Soc. Am.* 73: 909–929.

Rimer, N., T. Barker, S. Rogers, J. Stevens, and D. Wilkins (1994). Simulation of seismic signals from partially coupled nuclear explosions in cylindrical tunnels, Rep. DNA-TR-94-136, Defense Nuclear Agency, Alexandria, VA.

Stevens, J. L., T. G. Barker, S. M. Day, K. L. McLaughlin, N. Rimer, and B. Shkoller (1991). Simulation of teleseismic body waves, regional seismograms, and Rayleigh wave phase shifts using two-dimensional nonlinear models of explosion sources, AGU Geophysical Monograph 65: Explosion Source Phenomenology, S. Taylor, H. Patton, P. Richards, Eds., ISBN 0-87590-031-3, 239–252.

Stevens, J. L., N. Rimer, H. Xu, G. E. Baker and S. M. Day (2003). Near field and regional modeling of explosions at the Degelen Test Site, SAIC final report to DTRA, SAIC-02/2050.

Stevens, J. L., G. E. Baker, H. Xu, T. J. Bennett, N. Rimer and S. M. Day (2004). The Physical Basis of *Lg* Generation by Explosion Sources, SAIC Final Report submitted to the National Nuclear Security Administration under contract DE-FC03-02SF22676, December.

Stevens, J. L., S. Gibbons, N. Rimer, H. Xu, C. Lindholm, F. Ringdal, T. Kvaerna, and J. R. Murphy (2006). Analysis and simulation of chemical explosions in nonspherical cavities in granite, *J. Geophys. Res.* 111: doi:10.1029/2005JB003768.

Stevens, J.L and H. Xu (2008). Wave propagation from complex 3D sources using the representation theorem, in *Proceedings of the 30th Monitoring Research Review: Ground-Based Nuclear Explosion Monitoring Technologies*, LA-UR-08-05261, Vol. 1, pp 682–691.